

## Fabrication and characterization of *p-i-p* top-gate carbon nanotube FETs

Y. Noshō<sup>1</sup>, Y. Ohno<sup>1,2</sup>, S. Kishimoto<sup>1,3</sup>, and T. Mizutani<sup>1,4</sup>

<sup>1</sup>Dept. of Quantum Eng., Nagoya Univ., Furo-cho, Chikusa-ku, Nagoya 464-8603, Japan

<sup>2</sup>PRESTO/JST, 4-1-8 Honcho, Kawaguchi, Saitama 332-0012, Japan

<sup>3</sup>Venture Business Laboratory, Nagoya Univ., Furo-cho, Chikusa-ku, Nagoya 464-8601, Japan

<sup>4</sup>Institute for Advanced Research, Nagoya Univ., Furo-cho, Chikusa-ku, Nagoya 464-8601, Japan

Phone & Fax: +81-52-789-5387, E-mail: nosho@nagoya-u.jp

### 1. INTRODUCTION

Carbon nanotubes (CNs) are promising materials for the nano-scale electron devices such as CN field-effect transistors (CNFETs). In order to fully develop the potential of CNs, it is necessary to optimize the device structure [1]. In this study, we have fabricated *p-i-p* top-gate (TG-) CNFETs, where the access region was doped with F<sub>4</sub>TCNQ (tetrafluorotetracyano-*p*-quinodimethane) as *p*-type dopant [2]. This results in the improvement of device performance.

### 2. EXPERIMENTS

The schematic device structure and SEM image of the fabricated *p-i-p* TG-CNFETs are shown in Fig. 1 and Fig. 2, respectively. The single-walled carbon nanotubes were synthesized on a *p*<sup>+</sup>-Si wafer with SiO<sub>2</sub> (100 nm) by alcohol catalytic chemical vapor deposition [3]. After the formation of the source and drain electrodes, Au/Ti/AlO<sub>x</sub> top-gate structure was formed by electron-beam lithography, electron-beam evaporation, and lift-off process. The gate length (*l<sub>G</sub>*), gate insulator thickness (*t<sub>ox</sub>*), and source-drain distance (*l<sub>SD</sub>*) are 200 nm, 10 nm and ~3 μm, respectively. Finally, the access regions between the source and gate and between the drain and gate were doped with F<sub>4</sub>TCNQ as *p*-type dopant. The wafer was soaked in chloroform solution of F<sub>4</sub>TCNQ (3.6 mol/l) for 1.5 hours. We have confirmed the effectiveness of the F<sub>4</sub>TCNQ doping using back-gate-type (BG-) CNFETs. Figure 3 shows the *I<sub>D</sub>*-*V<sub>GS</sub>* characteristics of BG-CNFETs before and after the F<sub>4</sub>TCNQ doping. The threshold voltage (*V<sub>th</sub>*) shifted ~5 V toward positive *V<sub>GS</sub>*, and the on-current was increased 350% by the doping. The positive *V<sub>th</sub>* shift shows the effectiveness of F<sub>4</sub>TCNQ as a *p*-type dopant. The increase in on-current would be attributed to an increase of channel conductivity and/or a reduction of resistance of the Schottky contacts.

Figure 4(a) shows *I<sub>D</sub>*-*V<sub>GS</sub>* characteristics of CNFETs; BG-CNFET (dotted line), undoped TG-CNFET (broken line), and *p-i-p* TG-CNFET (solid line). Here, the substrate bias (*V<sub>sub</sub>*) was floating for the TG-CNFETs. In the case of both TG-CNFETs, subthreshold slope (*s*-factor) was improved to be 200 mV/dec as compared to that of BG-CNFETs (*s* ~ 1000 mV/dec). Another attractive property of the present TG-CNFETs is smaller hysteresis than that of BG-CNFET. In the case of BG-CNFETs, the large counterclockwise hysteresis has been related to water molecules [4] and organic contamination [5] around the CN channel. In the present TG-CNFETs, the active region is passivated by the gate oxide, resulting in the suppression of hysteresis. By the F<sub>4</sub>TCNQ doping, the on-current of TG-CNFETs was increased by one order of magnitude, and consequently, the *I<sub>on</sub>*/*I<sub>off</sub>* was improved to be 10<sup>3</sup> as shown in Fig. 4(b). The schematic energy band of *p-i-p* TG-CNFET is shown in Fig. 4(c). The F<sub>4</sub>TCNQ doping increases hole concentration in the access region. This results in a reduction of serial resistance of the access region.

### 3. SUMMARY

We have successfully fabricated F<sub>4</sub>TCNQ doped *p-i-p* TG-CNFETs. The top-gated device structure improved *s*-factor and reduced hysteresis, and the doping into the access region improved current driving capability.

### REFERENCES

- [1] J. Appenzeller *et al.*, IEEE Trans. Electron Devices **52**, 2568 (2005).
- [2] T. Takenobu *et al.*, Adv. Mater. **17**, 2430 (2005).
- [3] Y. Ohno *et al.*, Jpn. J. Appl. Phys. **42**, 4116 (2003).
- [4] W. Kim *et al.*, Nano Lett. **3**, 193 (2003).
- [5] H. Shimauchi *et al.*, Jpn. J. Appl. Phys. **45**, 5501 (2006).

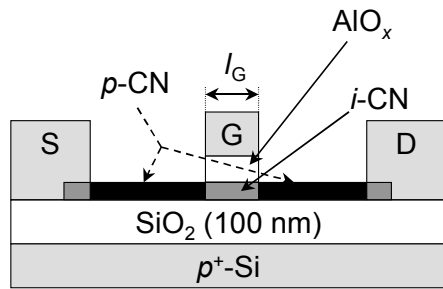


Fig. 1 The schematic device structure of F<sub>4</sub>TCNQ doped *p-i-p* top-gate (TG-) CNFETs.

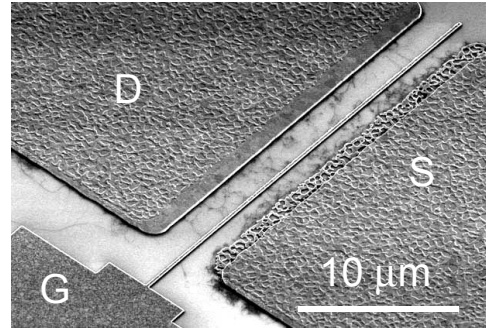


Fig. 2 SEM image of fabricated F<sub>4</sub>TCNQ doped *p-i-p* TG-CNFETs.

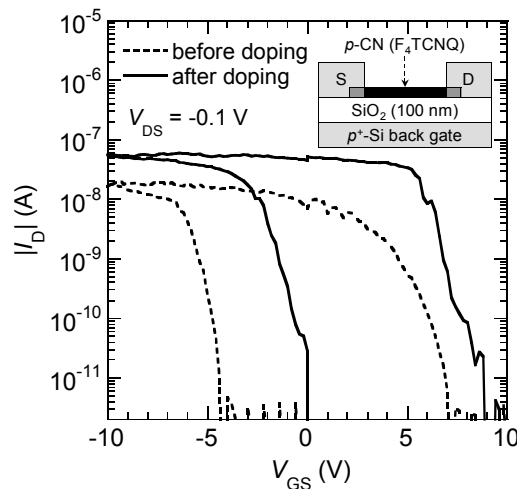


Fig. 3  $I_D$ - $V_{GS}$  characteristics of back-gate (BG-) CNFET before and after F<sub>4</sub>TCNQ doping. A  $V_{th}$  Shift toward positive  $V_{GS}$  and an increase in on-current were observed. Inset is the schematic device structure of *p*-doped BG-CNFETs.

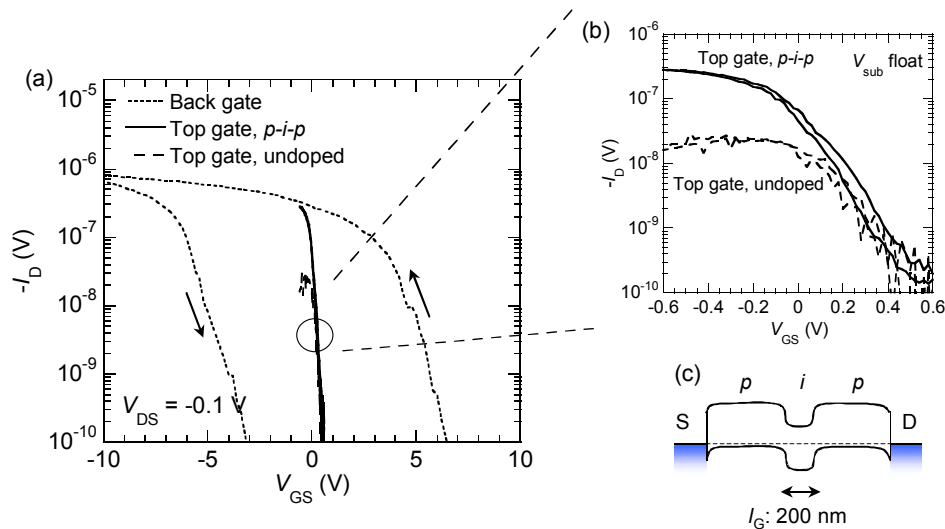


Fig. 4 (a)  $I_D$ - $V_{GS}$  characteristics of CNFETs; BG-CNFET (dotted line), undoped TG-CNFET (broken line), and *p-i-p* TG-CNFET (solid line). (b)  $I_D$ - $V_{GS}$  characteristics of TG-FETs. (c) Schematic band structure of *p-i-p* TG-CNFET. Subthreshold slope was improved and hysteresis were reduced by introducing the top-gate structure. The on-current of TG-CNFETs was increased by one order of magnitude by F<sub>4</sub>TCNQ doping.